PASSIVE AND ACTIVE STANDOFF INFRARED DETECTION OF BIO-AEROSOLS

C.M. Gittins, L.G. Piper, W.T. Rawlins, and W.J. Marinelli
Physical Sciences Inc.

James O. Jensen and Agnes N. Akinyemi
US Army ERDEC

Field Analytical Chemistry and Technology, **3**(4-5) (1999).

Report Documentation Page

Form Approved
OMB No. 0704-0188

1. REPORT DATE	2. REPORT TYPE	3. DATES COVERED
1999		**00-00-1999 to 00-00-1999**

4. TITLE AND SUBTITLE	5a. CONTRACT NUMBER
Passive and Active Standoff Infrared Detection of Bio-Aerosols	5b. GRANT NUMBER
	5c. PROGRAM ELEMENT NUMBER
6. AUTHOR(S)	5d. PROJECT NUMBER
	5e. TASK NUMBER
	5f. WORK UNIT NUMBER
7. PERFORMING ORGANIZATION NAME(S) AND ADDRESS(ES) **Physical Sciences Inc,20 New England Business Center,Andover,MA,01810**	8. PERFORMING ORGANIZATION REPORT NUMBER
9. SPONSORING/MONITORING AGENCY NAME(S) AND ADDRESS(ES)	10. SPONSOR/MONITOR'S ACRONYM(S)
	11. SPONSOR/MONITOR'S REPORT NUMBER(S)

12. DISTRIBUTION/AVAILABILITY STATEMENT
Approved for public release; distribution unlimited

13. SUPPLEMENTARY NOTES

14. ABSTRACT
see report

15. SUBJECT TERMS

16. SECURITY CLASSIFICATION OF:			17. LIMITATION OF ABSTRACT	18. NUMBER OF PAGES	19a. NAME OF RESPONSIBLE PERSON
a. REPORT **unclassified**	b. ABSTRACT **unclassified**	c. THIS PAGE **unclassified**		**29**	

PASSIVE AND ACTIVE STANDOFF INFRARED DETECTION OF BIO-AEROSOLS

C.M. Gittins, L.G. Piper, W.T. Rawlins, and W.J. Marinelli*

Physical Sciences Inc.

20 New England Business Center

Andover, MA 01810

James O. Jensen and Agnes N. Akinyemi

US Army ERDEC

ATTN SCBRD RTE / E5554

APG, MD 21010-5423

*Corresponding author.

ABSTRACT

Biological compounds are known to have infrared spectra indicative of specific functional groups. There is a strong interest in the use of passive means to detect airborne biological particles, such as spores and cells, which may act as biological weapons. At the sizes of interest, the infrared spectra of bacterial particles results from a combination of geometric ($\pi d_{particle} > \lambda$) and Mie ($\pi d_{particle} \sim \lambda$) scattering processes while the infrared spectrum of atmospheric particles falls into the Rayleigh limit ($\pi d_{particle} << \lambda$). In this paper we report on laboratory measurements of the infrared spectra of aerosolized *Bacillus subtilis* (BG) spores in air under controlled measurement conditions. Transmission measurements show an IR spectrum of the spores with features comparable to the condensed phase spectrum superimposed on a background of Mie scattering. Preliminary measurements indicate a peak extinction coefficient of approximately 1.6×10^{-8} cm^2 per spore at 9.65 μm. These results are discussed in terms of their implication for passive and active infrared detection and identification of bio-aerosols.

Keywords: LIDAR, scattering, biological, infrared, passive, extinction

1. INTRODUCTION

Vibrational spectroscopy of biological warfare (BW) agents has the potential to probe spores, vegetative cells, toxins, and rickettsia. In this paper we describe initial efforts to exploit the potential of vibrational spectroscopy to identify and determine the activity of BW agents. This approach utilizes extinction and scattering measurements to characterize the vibrational bands of bacterial particles. It may be possible to compare the vibrational band "fingerprint" of these materials to spectral libraries to afford rapid detection and identification of BW agents, as well as determine their activity. Though attempts have been made to interpret the infrared spectra of bacterial cells in terms of specific physical structures, the spectra exhibit the all the features of a multi-component mixture comprised of complex molecules.[1] Naumann has conducted an extensive review of the infrared spectroscopy of intact cells.[2,3] Of particular importance is the region from 1500 to 1700 cm^{-1} containing the so-called "amide I" bands, which are the strongest features in the spectra and contain information about the structures present in cell proteins. Spectra of apathogenic *Bacillus* strains show significant features at 1407 and 1605 cm^{-1}, which can be identified as symmetrical and asymmetrical carboxylate bands, as well as the strong amide I feature at 1653 cm^{-1} which can be linked to the presence of poly-D-glutamic acid in the capsule.

In this paper we discuss the results of preliminary measurements of the extinction coefficient for aerosolized *Bacillus subtilis var. niger* (BG) spores in the 2.7 to 12 μm wavelength region. We then relate those measurements to full IR spectrum measurements of thin films of BG. These measurements are coupled to calculations of Mie scattering for these particles in order to assess the role of scattering in the measured total extinction. The results of

these measurements and calculations are discussed in terms of their importance to both passive and active standoff biological agent detection.

2. EXPERIMENTAL MEASUREMENTS

2.1 Experiment Configuration

The measurements were conducted in an improvised aerosol chamber in the laboratories of Physical Sciences Inc. A schematic diagram of the configuration is shown in Figure 1. The chamber was a 32 x 32 x 80 in. high fiberglass and metal enclosure modified for optical access across its 32 in. depth. The BG spores were suspended in an aqueous solution and sprayed into the chamber utilizing an ultrasonic atomizer configured to deliver droplets with a mean diameter of 20 μm. The solution was metered to the atomizer using a peristaltic pump at a rate of 10 ml/min. A heated supply of ~ 50°C air was delivered to the chamber to break up the flow from the atomizer, prevent recondensation of water, as well as provide the heat of vaporization for the injected liquid. The flow rate was set to provide air in the chamber at approximately 50% relative humidity under ambient laboratory temperature conditions. The chamber pressure was held at ambient atmospheric through the use of a vent hose connecting the chamber to a fume hood. The chamber volume divided by the gas flow rate gives a characteristic residence time for gas in the chamber of approximately 3 min. A recirculating blower system was also available to provide a well mixed air flow in the chamber. However, we decided that the dilution flow provided ample mixing in the chamber and this blower was not used in most measurements because of concerns about sticking of particles in the blower system. Each change of chamber

operating conditions was allowed to equilibrate for 15 min (5 residence times) prior to conducting any optical measurements.

Optical transmission measurements were conducted in the chamber using a MIDAC FTIR spectrometer at a resolution of 16 cm^{-1}. The chamber afforded a single pass path length of 75 cm. Two inch windows on either end of the chamber were formed from 3M heat shrinkable polyethylene window insulation material. In situations where there is no pressure differential between the chamber and the ambient atmosphere this insulation was found to make a good window due to its low refractive index and lack absorption bands in the thermal infrared region (8 to 12 µm). Significant absorptions in the 3.3 and 6.5 µm regions make it unsuitable for some other investigations.

2.2 Sample Preparation And Concentration Determination

The BG spore samples were prepared from an existing stock simulant solution at U.S. Army ERDEC. Washed and unwashed samples were used in the reported measurements to assure the spectra observed were characteristic of the spores rather than residual growth medium or other contaminant. The spectra measured in this effort showed no difference between the washed and unwashed samples. The data reported in these measurements utilized an unwashed sample with a spore concentration of 8.8×10^9 ml^{-1} as determined by flow cytometry. In this paper we report extinction measurements on a per spore basis in order to avoid confusion about the extent of agglomeration in the aerosolization. In determining the spore concentration we assume steady state conditions. The spore aerosol concentration is simply given by dividing the spore injection rate (spores per minute) by the dilution air flow rate (cm^3 per minute). The spore injection rate is the product of the spore solution concentration (8.8×10^9 spores/ml) and the

liquid injection rate (10 ml/min) or 8.8 x 10^{10} spores/min. The gas flow rate was 1855 liters/min leading to a steady state spore concentration of 4.7 x 10^{4} spores cm^{-3}. Given a 75 cm optical path, the total column density for the measurements was approximately 3.6 x 10^{6} spores cm^{-2}. We note that the calculation of the steady state spore column density assumes no losses due to heterogeneous removal on the walls of the chamber. As such, the cross sections reported here are lower limits on the actual value.

2.3 Experimental Results

Spore aerosol measurements are conducted by bringing the chamber to steady state using pure water injection. Under these conditions a series of background spectra of the chamber are recorded for reference to the spectra recorded under spore injection. Following acquisition of the background the spore solution is injected into the chamber at the same flow rate as the pure water and the chamber allowed to equilibrate. Spectra of the aerosolized spores are then recorded and the chamber injection system returned to pure water. A series of post acquisition background spectra are recorded to account for baseline drift over the ~ 3/4 hour required for an acquisition sequence. Figure 2 shows a sequence of spectra recorded during the equilibration of the chamber following spore injection. The data clearly shows a broad feature growing in with a maximum at approximately 9.65 µm (1065 cm^{-1}) as well as additional features in the 3.1 µm (~3200 cm^{-1}) and 6.2 µm (~1620 cm^{-1}) regions. Under most conditions these features returned to baseline upon re-injection of the pure water solution. However, in some experiments spectral features were observed to persist following the changeover to pure water, probably indicating that window contamination had occurred. These data were not used in our analysis.

Good spore aerosol spectra could be reliably obtained throughout the IR region, except for the window absorption bands. The transmission measurements were used to determine the extinction coefficient. The spectra were converted to absorbance units (base e) using Beer's law. The absorbance data was converted to extinction cross sections using the column density assumed from the steady state analysis presented above. The results of this analysis are shown in Figure 3 for the region from 2.7 to 12 µm. The thin film transmission measurement is shown in Figure 4 as converted to absorbance units (base e). These measurements extend from 2 to approximately 14 µm. The spectral features are quite similar to the *Bacillus subtilis* spectra reported by Naumann[2].

3. DATA INTERPRETATION

3.1 Interpretation of Thin Film Spectra

The similarity between the thin film spectrum and the aerosol spectrum gives us some leeway in trying to relate the two pieces of data. The features in both spectra at 3.1 µm are clearly identified as the "amide A" bands.[2] The methyl stretching mode band in the aerosol spectrum is obscured by a window absorption band. Similarly, the "amide I" and "amide II" bands in the 5.5 to 8 µm region are also evident in both spectra, although partially obscured by another window absorption in the aerosol measurement. The feature at 9.65 µm can be attributed to bands associated with either a phosphodiester or polysaccharide.

To understand the utility of these features for standoff detection of bio-aerosols we also calculated the atmospheric transmission spectrum for a 10 km path at sea level and calculated the product of the two spectra to establish the spectral regions of utility for remote sensing applica-

tions. It is clear from the scaled data and the atmospheric transmission spectrum that the infrared regions from 8 to 13 µm and from 3.0 to 4.0 µm are key to standoff detection of the BG spore aerosols. Unfortunately, the region from 5.5 to 8.0 µm, which contains significant differentiating features in the spectrum, is obscured by atmospheric water absorptions. In the remainder of this paper we consider three standoff detection approaches: passive detection in the 8 to 12 µm band, active detection in the 9 to 11 µm region using CO_2 laser DIAL or DISC approaches, and differential scattering in the 1.5 and 3.5 µm region using the signal and idler from an OPO-based LIDAR system.

3.2 Passive Standoff Detection Approaches

The ability of a sensor to detect any biological or chemical cloud depends on the apparent radiance contrast due to the presence of the cloud compared to the noise-equivalent spectral radiance (NESR) of the sensor employed. In simple form, the relationship between the radiance contrast produced by the cloud and the sensor NESR is given by the expression:

$$\Delta N = \tau_{atm}\sigma_{spore}\rho\ K\Delta T \geq NESR \qquad (1)$$

where ΔN is the radiance differential due to the presence of the cloud, τ_{atm} is the atmospheric transmission between the cloud and the sensor (~65%), σ_{spore} is the absorption cross section on a per spore basis (1.6×10^{-9} cm^2 $spore^{-1}$), ρ is the spore column density, K is the derivative of the radiance with respect to temperature (~ 1.5×10^{-5} W cm^{-2} sr^{-1} μm^{-1} K^{-1}) at the sensor wavelength (9.65 µm), and ΔT is the apparent temperature difference between the cloud and the background. In these calculations we assume a low-sky ΔT of 21K. Typical sensor NESR values range from 10^{-6} to 10^{-7} W cm^{-2} sr^{-1} μm^{-1}. The differential radiance as a function of spore concentration is

shown in Figure 5 for a path length of 100 m through the cloud. The calculations show that the differential radiance does not exceed the sensor NESR until a spore concentration of ~4 per cm^3 is reached. Since the spores agglomerate to contain 2 to 10 spores per particle, the sensor NESR is reached at a particle density of 0.4 to 2 per cm^3. However, a significant fraction of the total cloud extinction is due to broad band scattering. Passive detection methods require that the sensor be able to sample the unperturbed background radiance from the scene at nearby wavelengths in order to assess the influence of the biological agent cloud on the transport of radiation from the scene to the sensor. This underlying broad band scattering component does not allow the sensor to sample the background radiance free of the influence of the agent cloud. Hence, as a practical matter the net observable radiance is probably limited to the structured absorption component of the total extinction cross section. This broadband component has the effect of reducing the contrast of the cloud in the scene by approximately a factor of two.

It is generally acknowledged that relevant bio-particle densities are in the range from 0.1 to 10 particles per cm^3. Hence, based on this preliminary assessment, passive sensing of a bio-aerosol cloud would appear to be at the limit of current passive detection capabilities Our calculations suggest field experiments should be conducted to assess the potential of these devices to detect bio-aerosols.

3.3 LWIR Disc/Dial Lidar

Differential LIDAR approaches generally require 10 to 20 percent absorbances to have reasonable sensitivity levels.[4,5] The transmission spectrum of the cloud from Figure 5 shows a 10% absorbance is not achieved in the 9.65 µm band until the number density exceeds approxi-

mately 1000 spores per cm^3. Hence, the DIAL approach in the long wavelength infrared (LWIR) is no more attractive than the passive sensor for most significant applications in bio-detection.

Differential scattering measurements in the LWIR are also difficult since the spore particle size is comparable to the scattering laser wavelength and the scattering efficiency is low. However, this size parameter regime, where the scattering and absorption properties of the aerosol are comparable, also provides an opportunity to use the absorption properties of the aerosol to aid in discrimination. The wavelength dependence of the volumetric backscatter coefficient is the key parameter in determining the ability of a LIDAR to discriminate natural from artificially introduced bio-aerosols. To obtain an initial assessment of the discrimination opportunity we have performed Mie Scattering calculations for the aerosol, using the measured extinction coefficients to assess the scattering and absorption components of the total extinction. The critical unknown in the calculation is the magnitude of the real refractive index for the spore particles throughout this wavelength range. In our calculations we have attempted to bound the problem using the real refractive index of water as a starting point for the calculation. The entire interaction process can be parameterized in terms of three coefficients: extinction (Q_e), absorption (Q_a) and scattering (Q_s). The measured extinction coefficient at 3.65 µm leads to a value of Q_e of approximately 1.5 for an assumed particle diameter of 3 µm comprised of approximately 6 spores. Using the Mie codes found in Bohren and Huffman[6] and assuming spherical particles, we can calculate Q_e as a function of possible values of the imaginary index (k), for a range of values of the real index (n). The calculation shows that, in the region of the measured Q_e at 3.45 µm, the inferred value of the real index is relatively insensitive to the assumed value of the imaginary index. We utilized an imaginary index of 0.20 and a real index of 1.3 in our calculations. The calculations assume the real refractive index is invariant with

wavelength and the imaginary index is determined from the measured value of Q_e at each wavelength considered.. Using this parameterization we can calculate the differential scattering cross section using the Mie codes. Although we have no extinction data at 1.55 µm, we expect the bio-aerosol absorption to be weak since this wavelength region is characterized by overtone and combination bands. Thus, we have assumed $k \approx 0$ at this wavelength.

A multi-mode log-normal distribution was used to parameterize both the biological and atmospheric aerosol distributions. The form of the distribution is given by:

$$n(r) = \sum_{i=1}^{n} \left(\left[\frac{N_i}{\ln(10)\ r\ \sigma_i\ \sqrt{2\pi}} \right] x\ \exp\left[-\frac{(\log\ r - \log\ r_i)^2}{2\ \sigma_i^2} \right] \right) \qquad (2)$$

where n is the number of modes, N_i is the fraction of the total distribution in each mode, r_i is the mode radius, and σ_i is the mode width. The angular scattering efficiencies were calculated for the biological and an atmospheric aerosol distributions defined in Table 1. The atmospheric aerosol distribution was the rural atmospheric aerosol model used in MODTRAN[7] which comprises a small radius water soluble fraction and a larger radius dust-like fraction. The biological aerosol distribution assumed a 1.5 µm mean radius, based on generally held opinions on the extent of agglomeration during spore distribution. The mode width was set to assure a negligible fraction of the distribution occurred at a size below the reported minimum width of a single spore (0.25 µm). Table 2 shows the values of the real and imaginary indices used in the scattering calculations for each wavelength.

Figure 6 shows the differential scattering cross sections ($cm^2\ sr^{-1}$) calculated for the log-normal bio-aerosol distribution defined in Table 1 at wavelengths of 1.55, 3.45, and 9.65 µm. A similar calculation was performed for the rural atmospheric aerosol model used in MODTRAN[7] to validate the scattering code. The bio-aerosol calculations correctly predict that the total

scattering cross section, as determined by integrating over all scattering angles, scales inversely with the scattering wavelength. However, the calculations show that virtually all of the enhanced scattering occurs in the forward direction (0 deg) while, in the backscattering direction important for LIDAR applications, there are only small differences in the cross section compared to the forward scattering.

The differential backscattering cross sections can be converted to volumetric backscattering coefficients (km^{-1} sr^{-1}) by assuming a particle number density and 1 km path length. The volumetric backscatter coefficients obtained from this calculation can be compared with values for the natural atmosphere for the same wavelengths.[7] Our code calculations were in good agreement with these values. The absolute and relative values of the coefficients have significance for LIDAR detection and discrimination capability. The comparison of the calculations (as a function of particle density) and natural atmospheric data are shown in Figure 7. The calculations seem to indicate a trend: the particle number density at which the volumetric backscatter coefficient for the bio-aerosol equals the natural background is inversely proportional to wavelength. However, the absolute value of the coefficients decrease with increasing wavelength. Thus, the ability to detect any aerosol signal improves at shorter wavelengths. However, the ability to detect a bio-aerosol against the natural background should improve at longer wavelengths.

Additional insight is obtained by comparing the ratio of volumetric backscatter coefficients as a function of wavelengths for the two different aerosols. This information is shown, normalized to the values at 1.55 µm, in Table 3. The initial conclusion from reviewing these ratios is that the OPO signal/idler ratio appears to provide little discrimination capability in LIDAR applications. Though there are significant differences in the total extinction cross

sections for the two wavelengths, these differences appear to manifest all in the forward scattering direction. However, the comparison also shows that some discrimination capability may be provided by comparing returns from a dual OPO/CO_2 LIDAR system, i.e., 1.55 versus 9.65 µm. This apparent discrimination capability may arise from two factors: 1) the sampling of a bio- aerosol distribution with a mean diameter of 3 µm compared to an atmospheric aerosol with a size distriubution centered around 0.1 µm, and 2) the enhancement of scattering in the region near the 9.6 µm absorption band in the bio-aerosol. Larger mean bio-aerosol radii would tend to enhance these size differences. However, we note that the inferred value of the real index measured at 9.65 µm (k = 0.39) is approximately 75% larger than the measurements of Querry reported by Flanigan.[8] The sensitivity of the scattering ratios to the measured value of the extinction coefficient at 9.65 µm suggests that confirmatory backscattering measurements are warranted.

4. CONCLUSIONS

The preliminary results reported in this paper are rendered significantly uncertain by a lack of understanding of the particle size distribution produced in the ultrasonic generator used to create the aerosol. Beyond the questions of aerosol generation, there remains a significant uncertainty in the actual particle/spore number density. The possibility of significant surface losses in the aerosol chamber makes the resulting extinction cross sections lower limits, at best. In future measurements we hope to include light scattering measurements which will provide a measure of actual particle size and density for extinction and laser backscattering measurements.

The existing data indicates that passive measurements of biological agent cloud may be quite difficult if the extinction cross sections determined in these measurements remain valid.

However, we again caution that these data represent lower limits to the actual extinction cross sections. The scattering calculations suggest that the signal/idler ratio in an OPO-based system may not provide the ability to discriminate natural atmospheric from bio-aerosols. However, the ratio of scattered intensities at 1.55 and 9.65 µm may provide that capability, albeit at difficult signal levels in the 9.65 µm band.

5. REFERENCES

1. D. Naumann, D. Helm, and H. Labischinski, "Microbiological Characterizations by FT-IR Spectroscopy," *Nature* 351, 81-82, (1991).
2. D. Naumann, C.P. Schultz, D. Helm, "What Can Infrared Spectroscopy Tell Us About the Structure and Composition of Intact Bacterial Cells," in *Infrared Spectrscopy of Biomolecules*, ed. by H.H. Mantsc and D. Chapman, Wiley-Liss, New York, 1996.
3. D. Naumann, D. Helm, H. Labischinski, and P. Giesbrecht, "The Characterization of Microorganisms by Fourier-Transform Infrared Spectroscopy (FT-IR)" in *Modern Techniques for Rapid Microbiological Analysis*, ed. by W.H. Nelson, VCH, New York, (1991), pp. 43-96.
4. F.M. D'Amico, "Quantitative Vapor Detection with a Multiwavelength CO_2 LIDAR," *Proc. of the 1996 Meeting of the IRIS Specialty Group on Active Systems*, 13-16 May 1996, pp. 345-364.
5. D. Dean, J. Blackburn, M. Fox, C. Hamilton, S. Alejandro, M. Stephen, S. Ghoshroy, Y. Weang, H. Stowe, M. Fava, J, DiMercurio, J. Dowling, M. Kelley, D. Senft, K. Agar, and M. Shilko, "Design of an Airworthy, Long-Standoff Range Differential Absorption

LIDAR Device," *Proc. of the 1996 Meeting of the IRIS Specialty Group on Active Systems*, 13-16 May 1996, pp. 365-384.

6. C. Bohren and D.R. Huffman, *Absorption and Scattering of Light by Small Particles*, John Wiley and Sons, New York, 1983.

7. A.S. Jursa, editor, *Handbook of Geophysics and the Space Environment*, National Technical Information Service No. ADA 167000, (1985). pp. 18-10 to 18-15.

8. D.F. Flanigan, *Hazardous Cloud Imaging: An In-Depth Study*, U.S. Army CRDEC Technical Report ERDEC-TR-416, July 1997.

Figure Captions

Figure 1. Schematic diagram of aerosol chamber and optical measurement system used for BG spore extinction measurements.

Figure 2. Time sequence of transmission spectra recorded during injection of BG spore sample into the aerosol chamber. The variable feature at 2350 cm^{-1} is due to atmospheric CO_2 absorption and is indicative of some baseline shift.

Figure 3. Extinction cross sections for aerosolized BG spores measured in this effort. Gaps in the spectrum indicate the location of window material absorption bands.

Figure 4. Absorption spectrum of a thin film of BG spores.

Figure 5. Differential radiance and optical transmission as a function of spore density in a 100 m cloud. Nominal NESR of typical passive sensor included for reference.

Figure 6. Calculated differential cross section as a function of scattering angle for wavelengths of 1.55, 3.45, and 9.65 µm.

Figure 7. Bio-aerosol and natural aerosol volumetric backscatter coefficients for the three wavelengths considered in this study. The bio-aerosol values are shown as a function of the cloud particle density for a 1 km path.

Tables

Table 1. Parameters Used in Defining Aerosol Distributions Used in the Scattering Calculations

Aerosol Model	Size Fraction (N_i)	Mode Radius (µm) (r_i)	Mode Width (µm) (σ_i)
Rural			
Water-soluble	0.999875	0.03	0.35
Dust-like	0.000125	0.50	0.4
Biological	1.000000	1.50	0.15

Table 2. Real (n) and Imaginary (k) Refractive Indices Used in the Scattering Calculations

	Wavelength (μm)					
	1.55		3.45		9.65	
Distribution	n	k	n	k	n	k
Rural Aerosol						
Water-soluble	1.50	2.0×10^{-2}	1.45	6.0×10^{-3}	2.60	0.4
Dust-like	1.37	9.0×10^{-3}	1.26	1.0×10^{-2}	1.70	0.15
Bio-aerosol	1.30	0.0	1.30	0.2	1.30	0.39

Table 3. Comparison of Relative Backscattering Coefficients and Size Parameters as a Function of Wavelength for the Two Aerosol Distributions

	Bio-aerosol		Atmospheric Aerosol	
Wavelength (μm)	Cross Section Ratio	Size Parameter ($2\pi r/\lambda$)	Cross Section Ratio	Size Parameter ($2\pi r/\lambda$)
1.55	1.00	3.87	1.00	0.13
3.45	0.27	1.74	0.42	0.06
9.65	1.05	0.63	0.19	0.02

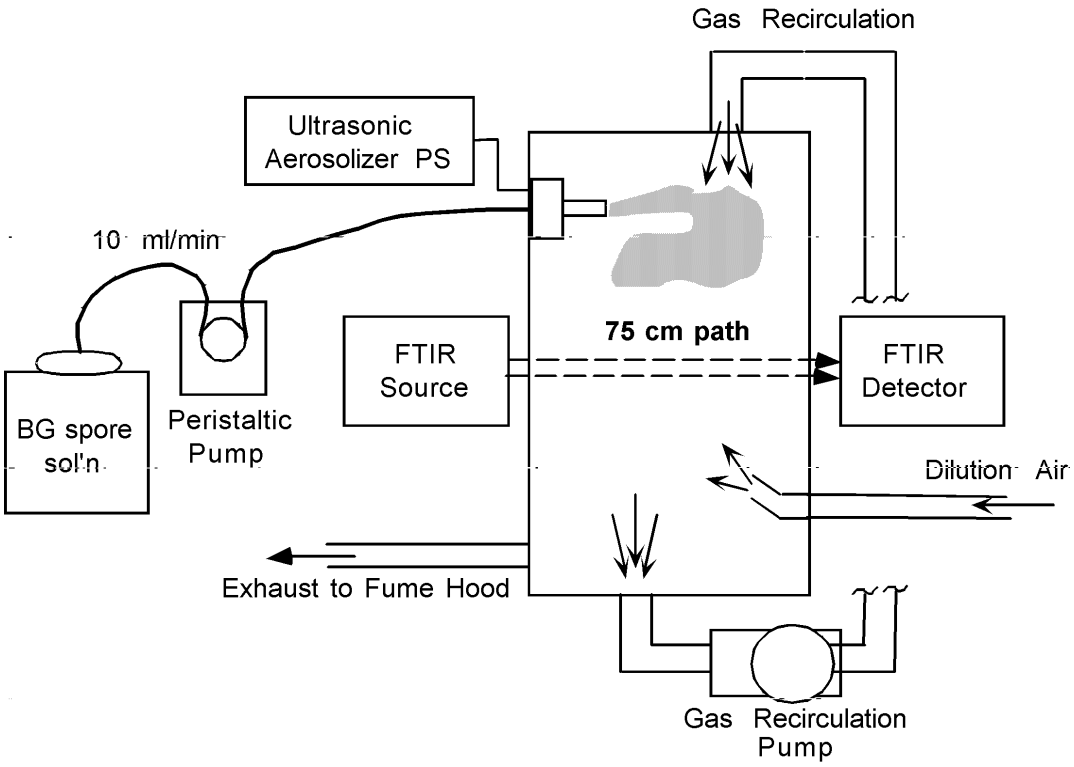
Gas Recirculation
Ultrasonic
Aerosolizer PS
10 ml/min
75 cm path
FTIR
Source
FTIR
Detector
BG spore
sol'n
Peristaltic
Pump
Dilution Air
Exhaust to Fume Hood
Gas Recirculation
Pump

Figure 1

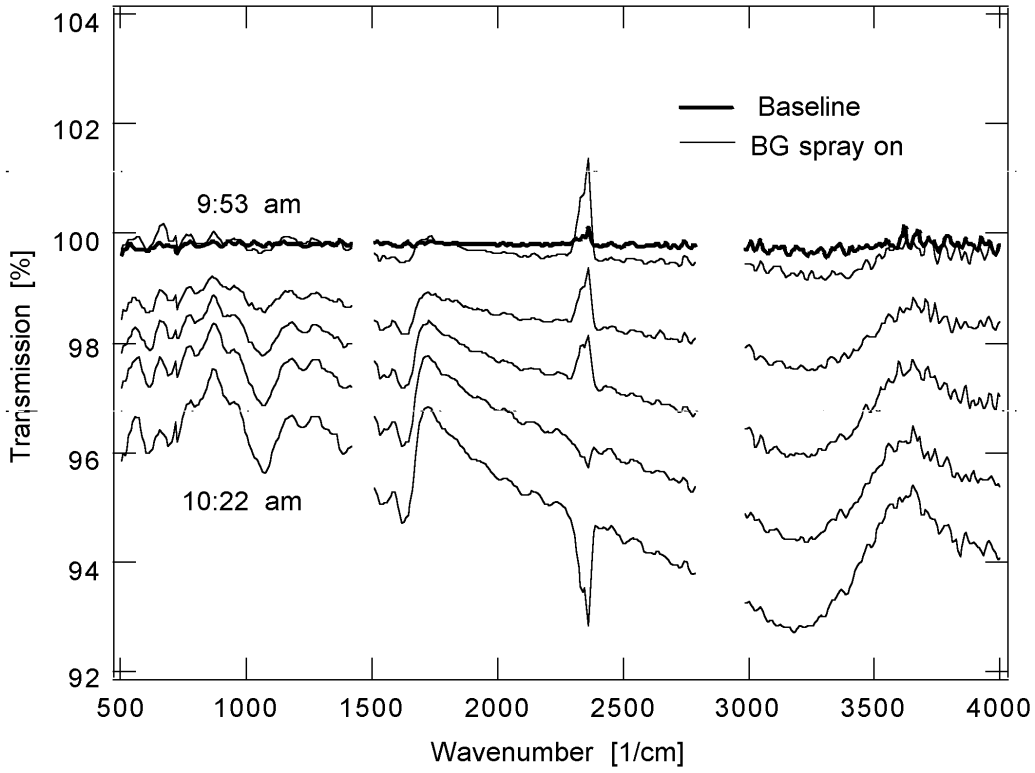
104
102
100
98
96
94
92
Transmission [%]
Baseline
BG spray on
9:53 am
10:22 am
500
1000
1500
2000
2500
3000
3500
4000
Wavenumber [1/cm]

Figure 2

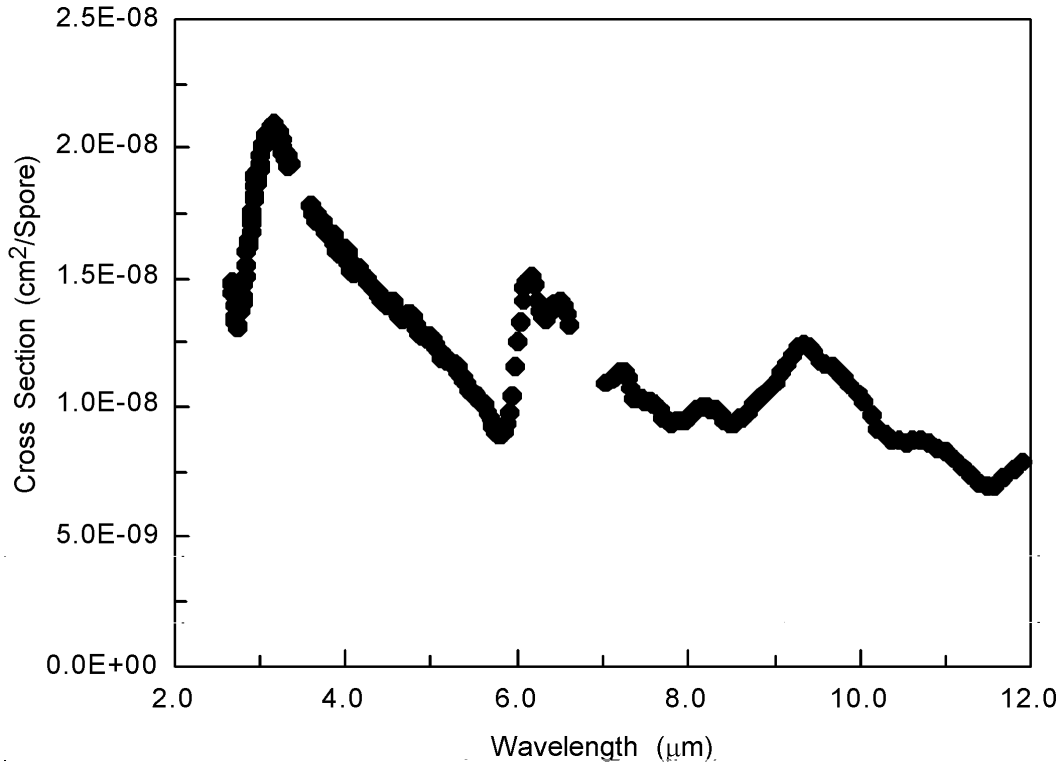
2.5E-08
2.0E-08
1.5E-08
1.0E-08
5.0E-09
0.0E+00
Cross Section (cm2/Spore)
2.0
4.0
6.0
8.0
10.0
12.0
Wavelength (μm)

Figure 3

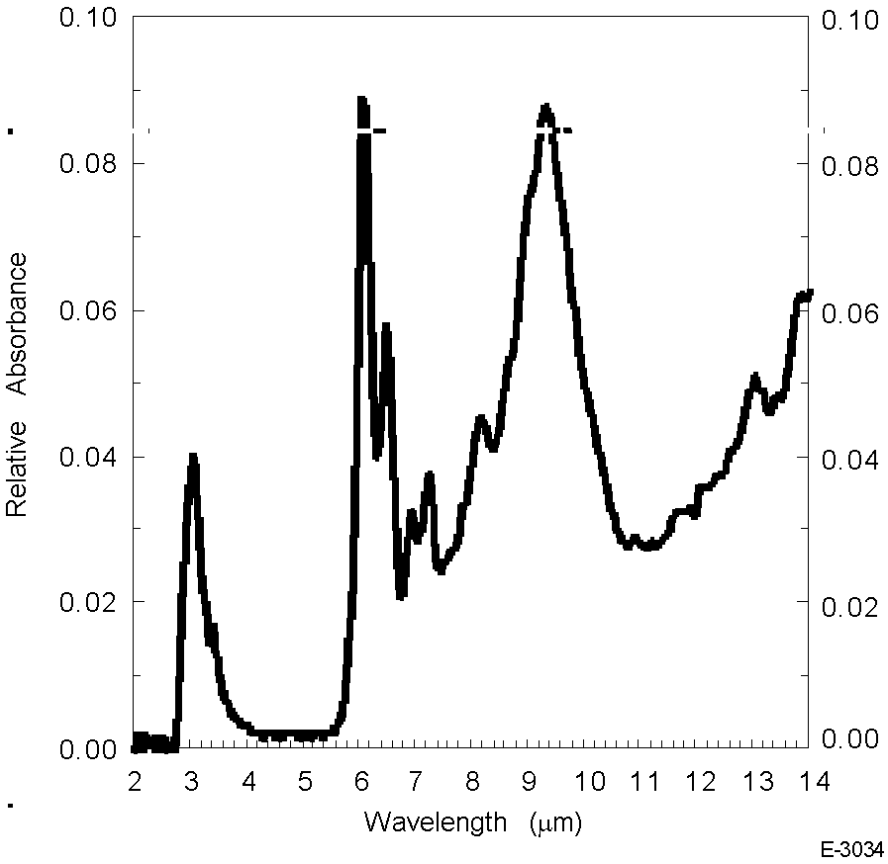
0.10
0.08
0.06
0.04
0.02
0.00
Relative Absorbance
2 3 4 5 6 7 8 9 10 11 12 13 14
Wavelength (μm)
E-3034

Figure 4

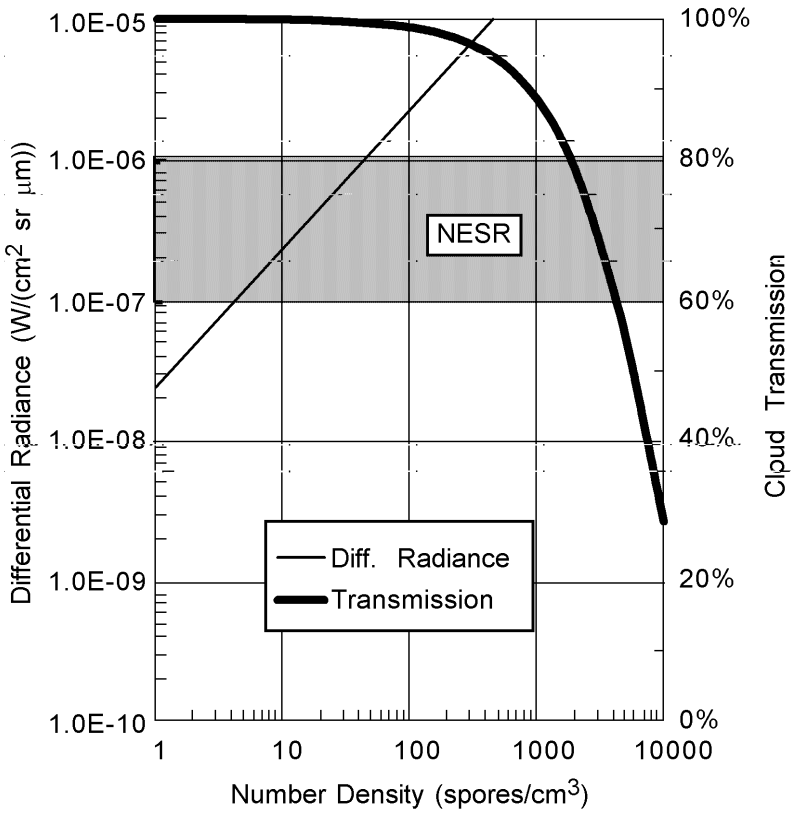
1.0E-05
1.0E-06
1.0E-07
1.0E-08
1.0E-09
1.0E-10
Differential Radiance (W/(cm2 sr μm))
100%
80%
60%
40%
20%
0%
Cloud Transmission
NESR
Diff. Radiance
Transmission
1
10
100
1000
10000
Number Density (spores/cm3)

Figure 5

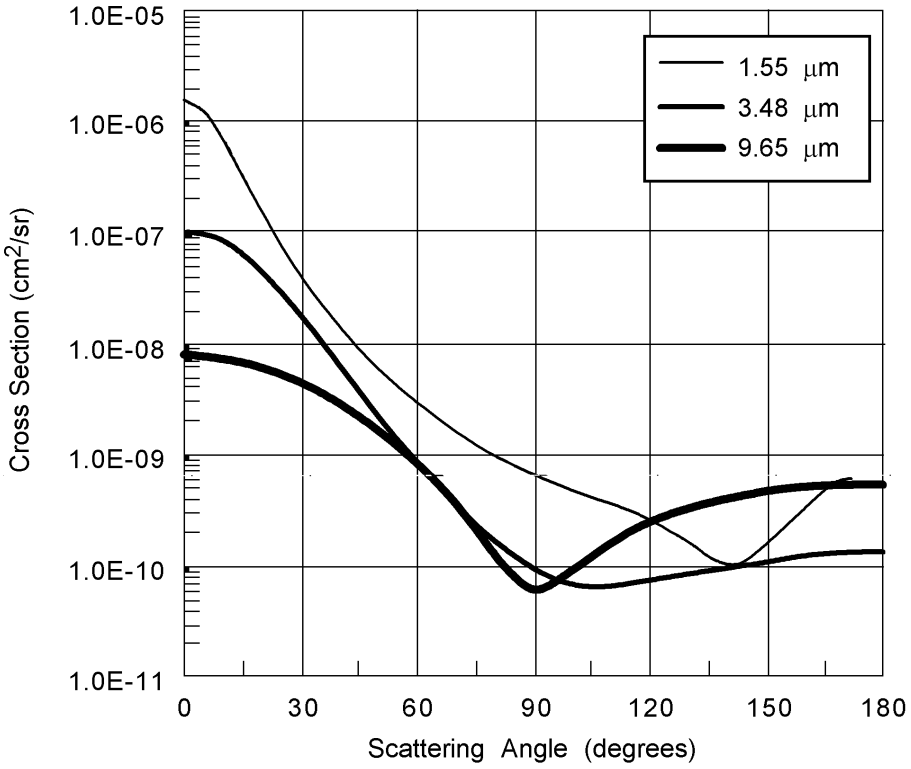
1.0E-05
1.0E-06
1.0E-07
1.0E-08
1.0E-09
1.0E-10
1.0E-11
Cross Section (cm2/sr)
0
30
60
90
120
150
180
Scattering Angle (degrees)
1.55 μm
3.48 μm
9.65 μm

Figure 6

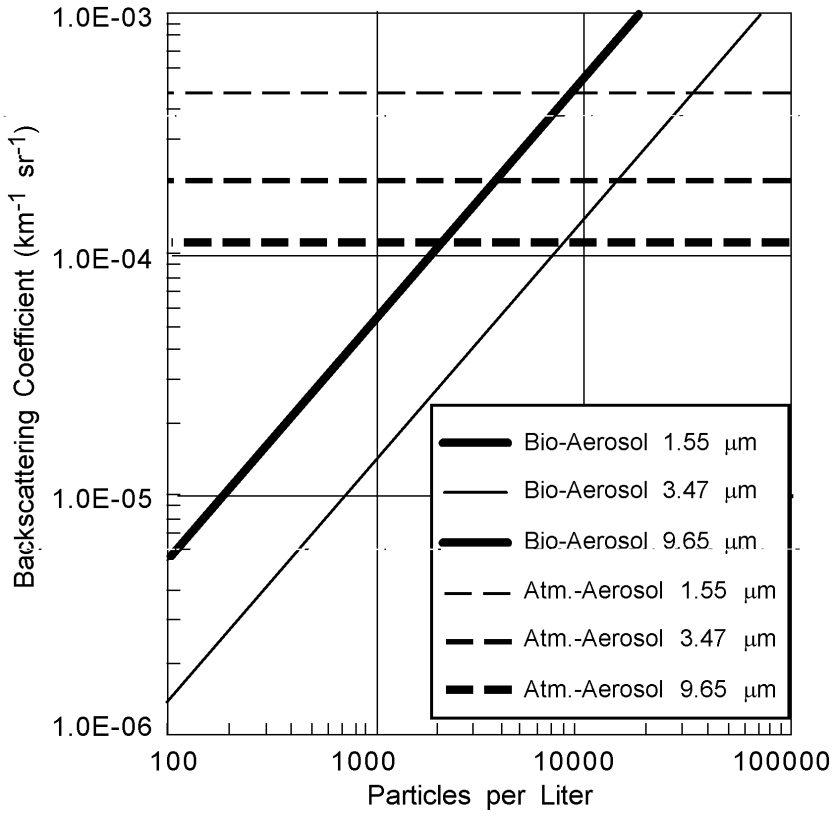
1.0E-03
1.0E-04
1.0E-05
1.0E-06
Backscattering Coefficient (km-1 sr-1)
100
1000
10000
100000
Particles per Liter
Bio-Aerosol 1.55 μm
Bio-Aerosol 3.47 μm
Bio-Aerosol 9.65 μm
Atm.-Aerosol 1.55 μm
Atm.-Aerosol 3.47 μm
Atm.-Aerosol 9.65 μm

Figure 7